ASPS Conference Proceedings 1: 1633-1640 (2022)

Proceedings of

12th Structural Engineering Convention-An International Event (SEC 2022)

Available at https://asps-journals.com/index.php/acp

Seismic Performance of Superelastic SMA Damper Retrofitted Building

S. Kashyap [1], S. Upadhyaya [2], S. Gur [3, *]

[1] Department Civil and Environmental Engineering, Master Degree Student, Indian Institute of Technology Patna, Bihta, Patna-801106, India
[2] Department Civil and Environmental Engineering, Doctoral Degree Student, Indian Institute of Technology Patna, Bihta, Patna-801106, India
[3] Department Civil and Environmental Engineering, Assistant Professor, Indian Institute of Technology Patna, Bihta, Patna-801106, India

Paper ID - 180471

Abstract

Nonlinear dampers are well known retrofitting system for the building structure, to mitigate seismic hazard. In past, among different type of nonlinear dampers, metallic yield dampers gain significant attention due to its high energy dissipation capacity. However, it has been observed while yield damper reduces floor displacement, but increases floor acceleration and leaves large residual displacement at the end of ground motion. Present study focuses on the application of shape memory alloy (SMA) dampers as an alternative to the yield damper, for retrofitting of building structure under seismic loading. Thus, response analyses are performed for nonlinear building structure without and with yield damper or SMA damper, under a large number of ground motion. Vibration control efficiency of yield and SMA damper are estimated in terms of the absolute maximum values of the floor acceleration, interstory drift ratio, and residual displacement. Response parameters are estimated over wide range of parameters of damper, building structure, and ground motion. Parametric study results revealed that yield damper provides very less acceleration control efficiency and some of cases it become more than uncontrolled structure. In contrast SMA damper slightly improves the acceleration control than yield damper (almost 14 %). In Comparison to the yield damper, SMA damper reduces the interstory drift ratio by 38 % and residual floor displacement by 47 %. Therefore, SMA damper provides major advantage in floor displacement reduction over yield damper, and acts as better re-centring device for seismic retrofitting application

Keywords: Yield Damper, SMA Damper, Nonlinear Analysis, Seismic Loading, and Building Retrofitting

1. Introduction

Construction of sustainable and resilient building structures is an important issue in structural engineering. Specifically, modern cities are coming up with closely spaced high rise buildings structures, putting them at risk of catastrophic and cascading failure in case of intense seismic event. In past, during major earthquakes (such as Mexico City 1985, Loma Prieta 1989, and Northridge 1994), substantial damage and failure of building structures has been reported [1–3]. This leads to the development of a very widely accepted idea of vibration control or retrofitting the building structures using dampers and subsequently it has been frequently used in the civil engineering structures. Seismic response of structures could be controlled in four ways such as active, semi-active, passive or hybrid control systems. Active or semi-active control system needs direct participation of energy source, whereas passive damper doesn't prerequisite the same and as well as they are mostly inexpensive. In past studies, many researchers reported that among different type of passive dampers, metallic yield damper (made of steel, aluminium, copper etc.) provide more stable hysteresis behaviour and dissipate large amount of input seismic energy [4]. It has been found that, optimal configuration and placement of metallic damper effectively reduces the seismic response of structure [5]. However, the metallic yield damper results a large residual deformation after an earthquake. Hence, study recommended to provide some clearance at this damper location [6], however, the solution to the residual deformation is more pronounced in case of post-earthquake scenario. Other studies proposed many different types of recentering devices to minimize interstory drift, however they leave permanent deformation. Thus, the post-seismic event residual drifts in yield damper increase the building retrofitting cost.

To overcome this, a novel material shape memory alloy (SMA) can be used because of the characteristics of pseudo-elasticity [7]. Pseudo-elastic property is the ability of SMA to regain its original shape due to the microscopic orientation of the molecules, under the thermo-mechanical loading. Many in-depth studies are conducted to explore this material in the structural engineering field [7–9]. SMA (specifically NiTi) can recover a large inelastic strain (up to 8% strain) by the phase transformation process. Graesser-Cozzarelli proposed a SMA material model for the seismic retrofitting application [8] and subsequently explore the phase transformation (PT) process in the SMA. PT can be temperature induced i.e. shape memory effect (SME) or stress induced super-elasticity (SE). There are mainly two phases in SMA i.e., austenite and martensite. Due to thermo-mechanical loading at room temperature, SMA material

*Corresponding author. Tel: +916115233819; E-mail address: sgur@iitp.ac.in

Proceedings of the 12th Structural Engineering Convention (SEC 2022), NCDMM, MNIT Jaipur, India| 19-22 December, 2022

Published online: December 19, 2022
doi:10.38208/acp.v1.699

transform from the austenite to martensite phase and upon unloading comes back to its original shape via complete martensite austenite PT.

Double X type SMA damper is studied for post-earthquake serviceability in bridge pier [10]. The restoring and energy dissipating behavior of SMA are verified in this study. Similar behavior of SMA is examined by reinforcing NiTi wires in a steel braced frame [11]. SMA wires-based dampers has been studied for vulnerability reduction in the braced frames [12]. Except SMA wires and bars, SMA rings are also utilized as damper device and the symmetry of single and dual rings have been also studied [13]. Cyclic tension compression tests on recentering SMA damper are performed and validated via newly proposed and improved Graesser-Cozzarelli model of SMA [14]. Martensitic hardening is an important phenomenon and frequently occurs when structure is subjected to extreme loadings with a high amplitude. Hence, to incorporate this aspect, the modified Wilde SMA material model (an extra back stress expression) is used by the above researcher. For tension-only SMA devices, degradation and loss of super-elasticity has been observed. Thus, to enhance its efficiency, novel SMA damper is proposed where two group of SMA bars are used to work together, one being in compression and other at tension simultaneously [7]. Similar behaviour of SMA dampers under compression and buckling are studied by different researcher [15,16]. Another study proposes a reusable hysteretic damper via adjusting various design parameters, which can withstand strong earthquake motions [17]. Among various parameters, the training effect of SMA has been also explored in previous study [18]. Whereas other research [19] suggest pre-tensioning the SMA rods could provide greater dissipation of input energy and better re-centring capability. Though many design methods are proposed for improving buckling of SMA damper [14], one study suggested that, the SMA dual rings under bending with compression or tension can be more promising for vibration reduction [13].

As it can be found, the aforementioned studies are more based on simpler model on SMA where the thermo-mechanical properties are not incorporated. The damping behavior of SMA is operated through its energy dissipation capacity, as described in previous study [9]. Other studies used thermo-mechanical material model of SMA [20,21] and suggested that, the energy dissipation (i.e. area under hysteresis curve) directly depends on temperature and strain rate. These two parameters can be captured by using the thermomechanical model. Moreover, most of the literatures discussed the design parameters of SMA damper to achieve better hysteresis and recentering behavior. Similarly, the yield dampers are discussed for optimum placement and design parameters for better response control. However, comparative study on yield and SMA damper performance under varying parameters of damper, structure, and seismic excitation is scant. Hence this study is motivated to put forward the comparison of both the dampers as seismic retrofitting devices and their efficiency for vibration control of nonlinear building structure under seismic loading. To capture the material model non-linearity of building structure and yield damper, parametric Bouc-wen model has been used [22]. For material model of SMA damper, a 1-D thermo-mechanical constitutive relation is used, which capture the temperature and strain rate effect of SMA [23]. Nonlinear time history analyses are carried out to determine the floor acceleration and displacement responses of the damped retrofitted building, and compare with uncontrolled building. Parametric study is performed for varying normalized strength of damper, time period of the building structure, and peak ground acceleration (PGA).

2. Material Modeling of Building and Dampers

This section discusses the material modelling details of the building, yield dampers and SMA dampers. In the present study, building is modelled to capture nonlinearity and dampers are also modelled using the nonlinear material models as discussed below.

2.1 Material Modeling of Building and Yield Damper

Mechanical model of yield damper has been shown in Fig. 1 (a), and corresponding hysteresis loop of yield damper is provided in Fig. 1 (b). In this present study, to represent nonlinear force-deformation hysteresis behavior of steel building frame and yield damper, parametric Bouc-Wen model is used. Fig. 1 (b) show the bi-liner force-displacement curve to depict the hysteresis behavior of the building and yield damper, as modeled via Bouc-Wen material model [22]. These hysteresis loops dissipate a significant part of input energy and the material model successfully simulates the non-linear force deformation characteristics of steel material and is expressed in Eq. 1 and 2.

$$F_z(x, Z) = (k_d + \alpha_z k_z)x + (1 - \alpha_z)F_{yz}Z \quad (1)$$

$$\dot{Z} = \left(\frac{\delta}{q_z}\right)\dot{x} - \left(\frac{\gamma}{q_z}\right)|\dot{x}|Z|Z|^{\eta-1} - \left(\frac{\beta}{q_z}\right)\dot{x}|Z|^{\eta} \quad (2)$$

Here, F_z is the restoring force, k_d is the liner stiffness of the yield damper, k_z represents the initial elastic stiffness, α_z is the post to pre yield stiffness ratio (i.e., rigidity ratio), F_{yz} and q_z are the yield strength and displacement, x and $\dot{x}$ are the relative displacement and velocity, and variable Z is the non-dimensional parameter, represents the hysteretic behavior of metallic material. Parameters δ, γ, β and η controls the shape and transition (elastic to plastic) of the hysteresis loop.

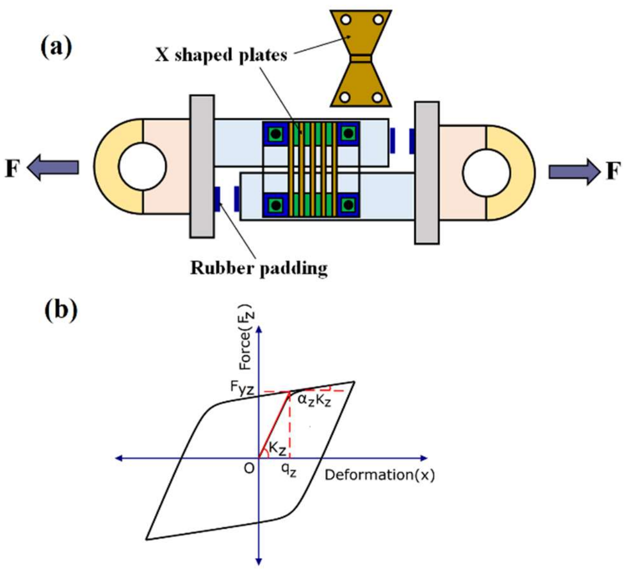

Fig. 1: (a) Mechanical model of yield damper and (b) Bouc-Wen hysteresis model for the building and yield damper.

2.2 Material Modeling of Superelastic SMA Damper

Fig. 2 (a) provides the mechanical model of SMA damper, and here two SMA wires are connected at front and back side of the sliding surface. Fig. 2 (b) shows flag shaped force-deformation behaviour of super-elastic SMA, as modelled via the thermo-mechanical constitutive relation [21,23]. Also Fig. 2 (b) shows that, the SMA's hysteresis loop is big enough for significant energy dissipation, as well as it has almost no residual displacement after the unloading. Two important characteristics of SMA are shape memory effect (SME) and super-elasticity (SE) which are controlled via thermo-mechanically induced phase transformation process, from austenite to martensite phase and vice versa. SMA stays in austenite phase above the austenite finish temperature (A_f) and upon loading austenite transform into martensite. During unloading, martensite transforms back to austenite, resulting dissipation of energy through the flag-shaped hysteresis loop and leaving no residual deformation. This shows the re-centring ability of the superelastic SMA. However, below A_f temperature, after the unloading, SMA leaves large residual deformation, which can be recovered by heating above A_f.

In this study Helm and Haupt SMA material model is adapted to simulate the material modelling of SMA damper. This model can capture the thermo-mechanical behaviour of SMA considering SME and SE effect. Further, the model has been experimentally verified to depict all the essential characteristics of the SMA material. Following the previous studies [21,24], the 1-D force-deformation material model of SMA is expressed as

$$F_s = (k_d x) + \left(\frac{F_{ys}}{q_s}\right)\left[(x - x_{in}) + \left(\frac{9\alpha k L_s}{4\mu + k}\right)(T - T_0)\right] \quad (3)$$

Here, F_s is the restoring force in the SMA spring, k_d is the liner stiffness of the SMA damper, F_{ys} and q_s are the phase transformation strength and displacement of SMA, k is the bulk or compression modulus (= 43, 000 MPa), μ is the shear modulus (19800 MPa); α is the linear thermal expansion coefficient (1.063×10^{-5} 1/K); x and x_{in} are the applied displacement and developed inelastic displacement, L_s is length of SMA spring, and T is the temperature of SMA and T_0 is the ambient temperature.

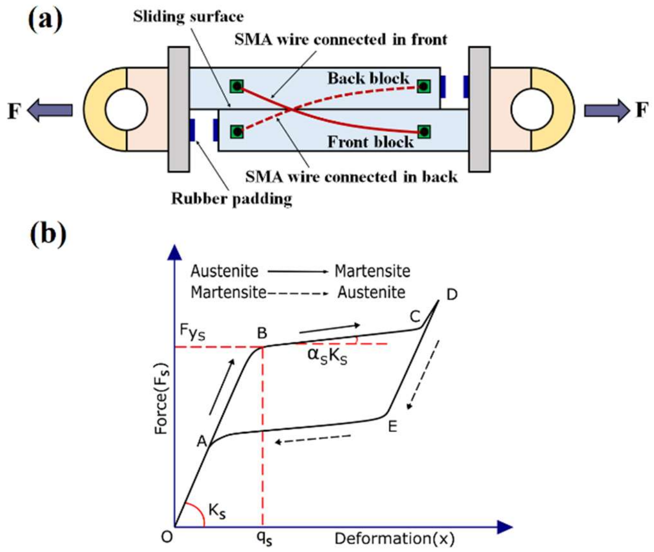

Fig. 2: (a) Mechanical model of the SMA damper and (b) force-deformation hysteresis model of the SMA damper.

3. Analysis and Simulation Process

Details of the analysis and simulation process are discussed in this section. It covers the formulation of equation of motion of the nonlinear building-damper system and the ground motion details.

3.1 Numerical Modeling

In this study, for the numerical simulation, a 2-D seven story steel frames building idealized as nonlinear shear buildings is adopted. Material non-linearity in the building model has been incorporated through the parametric Bouc-Wen model. To study the response control efficiency of yield or SMA dampers, they are connected at every floor, starting from first floor to seventh floor. Since, the yield dampers and SMA dampers dissipate significant part of seismic energy, thus they behave nonlinearly and accordingly modelled via parametric Bouc-wen material model for the yield damper and thermo-mechanical material model for the SMA damper. Fig. 3 (a) and (b) shows the idealized model of the building retrofitted with yield damper and SMA damper, respectively.

Considering building and damper to be nonlinear, on the basis of force equilibrium, following equation of motions are derived for the building with yield damper (Eq. 5) and SMA damper (Eq. 6) system, respectively

$$\begin{aligned}[M]\{\ddot{x}\} + [C]\{\dot{x}\} + [K + K_d + K_{yd}]\{x\} + [F_h]\{z\} \\ + [F_{hyd}]\{z_{yd}\} = -[M]\{r\}\ddot{u}_g\end{aligned} \quad (5)$$

$$\begin{aligned}[M]\{\ddot{x}\} + [C]\{\dot{x}\} + [K + K_d + K_{sd}]\{x\} + [F_h]\{z\} \\ + [F_{hsd}]\{x_{in}\} + [F_{Tsd}]\{r\} \\ = -[M]\{r\}\ddot{u}_g\end{aligned} \quad (6)$$

Here $[M]$, $[C]$ and $[K]$ are the mass, damping and stiffness matrix of the nonlinear building, respectively; $[K_d]$ is the linear elastic stiffness of the damper; $[K_{yd}]$ and $[K_{sd}]$ are the elastic stiffness part of the yield damper and SMA damper, respectively; $[F_h]$ is the non-liner hysteresis force of the building column; $[F_{hyd}]$ and $[F_{hsd}]$ are non-linear hysteresis force matrix of the yield damper and SMA damper, $[F_{Tsd}]$ is the developed force in SMA damper due to the temperature variation. The column vector of displacement, velocity and acceleration at each floor level of the non-linear building are represented as $\{x\}$, $\{\dot{x}\}$ and $\{\ddot{x}\}$; $\{z\}$ vector represents

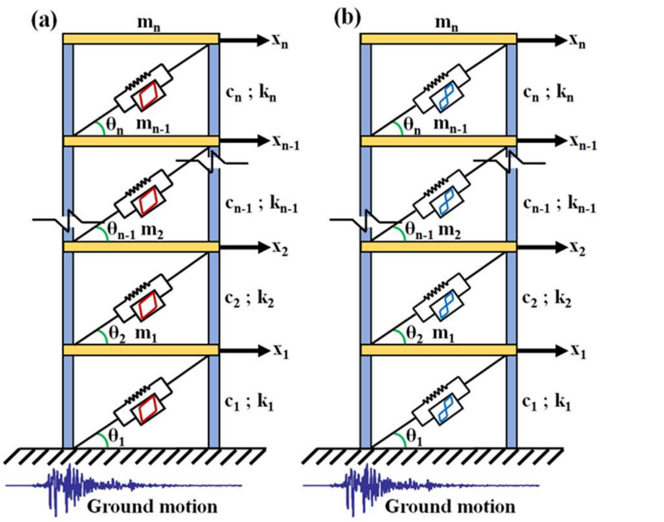

Fig. 3: (a) Idealized model of building structures connected with (a) yield damper and (b) super-elastic SMA damper.

the hysteresis DOFs of the building; $\{z_{yd}\}$ is the hysteresis DOFs of the yield damper; $\{x_{in}\}$ is the inelastic displacement DOFs of the SMA dampers; $\{r\}$ is the influence coefficient vector; and $\ddot{u}_g$ is input ground motion.

Response of the building with or without dampers (yield or SMA) under ground motion is obtained by solving the nonlinear system of equations. The nonlinear equation of motion of building or building-damper system is solved via step-by-step iterative process, i.e. Newmark-beta (average acceleration) integration method. At every time step and every iteration process, fourth order Runge Kutta method has been used to predict the nonlinear force in building column and yield or SMA dampers. As the building and dampers both are modelled to go into nonlinear regime, and therefore the equation of motions with the nonlinear material models are solved iteratively considering a very small-time step i.e. $\Delta t = 0.0001$ second. At every time step, multiple iterations are performed to get most accurate results and iterations have been continued until the difference between two consecutive iterative solutions become less than a tolerance limit ($\delta_{tol} = 10^{-5}$). Note that, all these values and process of simulation steps are adopted from relevant previous studies [21,24,25].

3.2 Ground motion selection

Response output of any nonlinear dynamic analysis of building structure strongly depends on the characteristic of the input ground motion. Some of the very recent studies already demonstrated that the traditional control system loses its control efficiency under strong ground motions, due to the presence of long-period and high-amplitude velocity pulses.

Thus, coincident of the time period of velocity pulses and the controlled buildings, it can trigger the resonance phenomena, which ultimately can cause substantially damage to building structure. Therefore, in this present study, a total of 25 ground motions are selected for numerical simulation, considering both near-fault and far-fault types. During the selection of ground motion, consideration has been put to capture a wide range of variations in PGAs (0.07g to 1.50g), PGVs (0.05 m/s to 1.25 m/s), and the dominant frequency contents (0.18 s to 1.72 s), which primarily depicts response behaviour of the building structure. Fig. 4 shows the spectral acceleration of the selected ground motions under varying time period of structure and 2% damping ratio.

4. Results and Discussion

This section provides the results of nonlinear time history of only building and retrofitted building (via yield and SMA dampers). At first the response analysis is performed to establish the control efficiency of yield damper and SMA damper, followed by parametric studies. For the simulation process, default value of different parameters are adopted as, for the building time period = 0.625 s (floor mass = 300 kg and stiffness = 795 kN/m) damping ratio = 3.0 %, normalized yield strength of building column = 6.0, post-to-pre yielding stiffness ratio = 2.0 %, and hysteresis loop parameters for the building column $\delta = 1.0, \gamma = \beta = 0.5,$ and $\eta = 10.0$; for yield damper stiffness ratio = 0.15, normalized yield strength = 0.05 with the yield displacement = 0.0025 m, post-to-pre yielding stiffness ratio 0.05, and hysteresis loop parameters $\delta = 1.0, \gamma = \beta = 0.5$, and $\eta = 1.0$; finally, for SMA damper stiffness ratio = 0.15, normalized transformation strength of SMA = 0.05 with the transformation displacement = 0.0035 m, length of SMA wire = 0.35 m, and ambient temperature = 300 K. In this study, values of different parameters are adopted from previous studies [24,25].

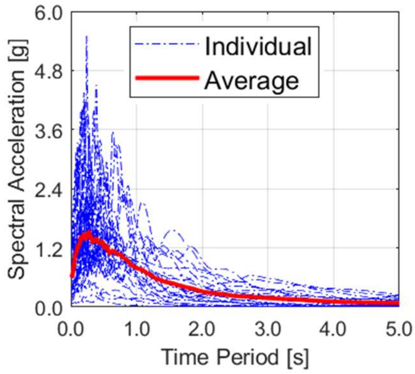

Fig. 4: Spectral acceleration of selected ground motions

The parameters of both the dampers and the damper location are adopted in such a way that they will produce minimum peak floor interstory drift ratio and residual displacement. Thus, the dampers are connected in all the floors of the building structure. Here for simulation purpose, a seven-storey nonlinear steel building frame represented is adopted and modelled as shear building. At first the nonlinear shear building is analysed in uncontrolled state and then via yield or SMA damper retrofitted condition. In retrofitted state of the building, yield or SMA damper are connected at every floor level.

Fig. 5 shows the nonlinear time history analysis results for uncontrolled and yield or SMA damper retrofitted buildings, under Imperial Valley earthquake (10/15/1979 station and component ElCentro array #5, 230). Fig. 5 (a) and (b) shows the response of the top floor acceleration and top floor interstory drift of the building structure. It can be observed that, compare to the uncontrolled building, yield and SMA damper retrofitted building shows reduction in the top floor peak acceleration by 9.5 % and 23.4 %, respectively. Similarly, the top floor interstory drift reduction in retrofitted building is 8.1 % for yield damper supplemented case, and 15.7 % for SMA damper supplemented case. A very important observation is the large residual displacement reduction efficiency of the SMA damper over yield damper. Due to the re-centring capability of SMA material, at the end of ground motion, SMA damper retrofitted building leaves almost no or very less residual displacement. In comparison to the uncontrolled building, yield damper and SMA damper reduces the residual displacement by 18.1 % and 43.5 %, respectively. Fig. 5 (c) shows the bi-linear hysteresis loop of the nonlinear building column. For uncontrolled and yield damper retrofitted building shows a permanent deformation at the end of earthquake. But, due to the shape recovery property of SMA material, in case of the SMA retrofitted building, it shows complete recovery of floor displacement, after the ground motion. Force displacement hysteresis loop for the yield damper (bi-linear) and the super-elastic SMA damper (flagged shape) are shown in Fig. 5 (d). Here also hysteresis loop of yield damper shows the large residual displacement, whereas super-elastic SMA damper shows almost no or negligible amount of residual displacement. Fig. 5 (e) shows the evolution of stress induced martensite phase fraction in SMA damper, and this is primarily responsible for the complete shape recovery of SMA material.

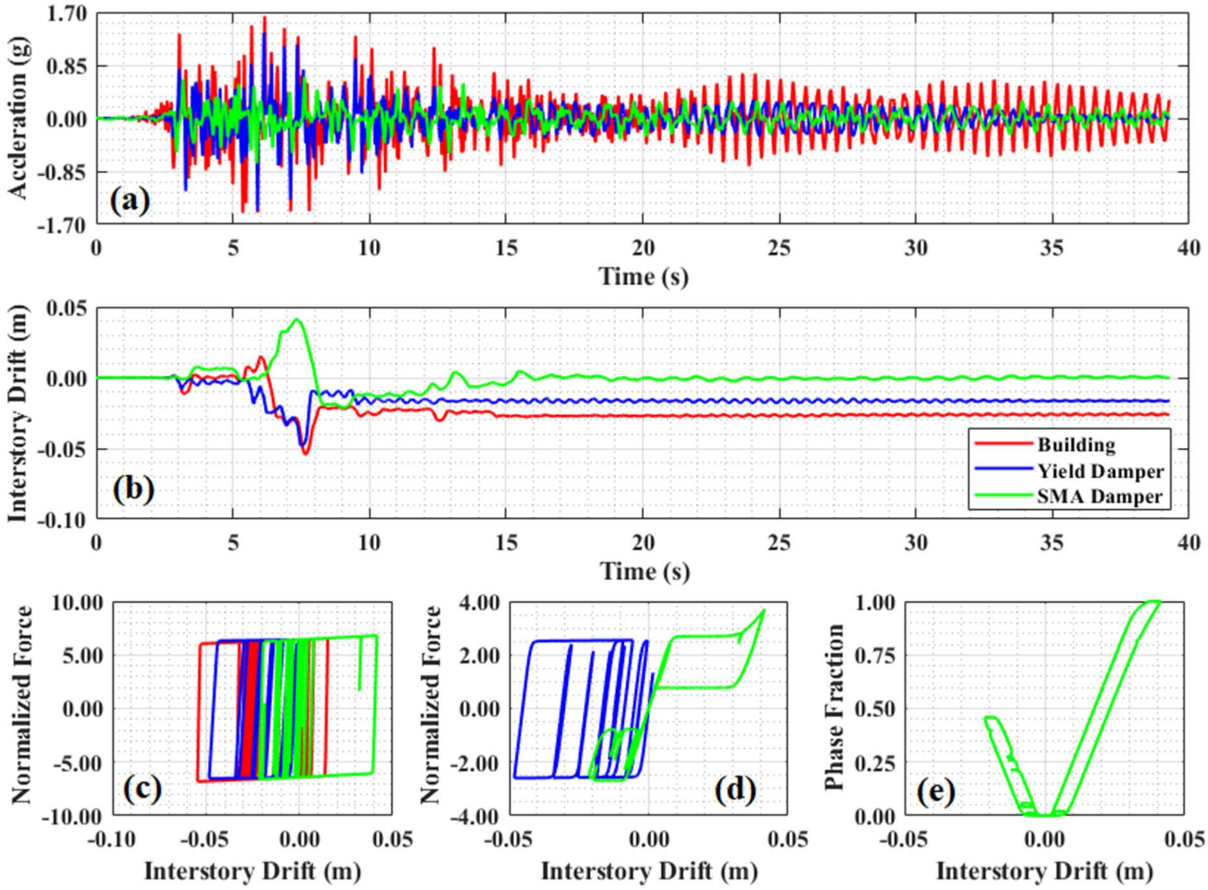

Fig. 5: Time history response results of top floor (a) acceleration and (b) interstory drift of the building structure, without and with yield or SMA dampers retrofitted case, under the Imperial Valley earthquake (10/15/1979, station ElCentro array #5, 230). Force displacement hysteresis loop of (c) building column and (d) yield or SMA damper. (e) Evolution of martensite phase fraction for SMA damper.

Fig. 6 demonstrate the effect of damper strength (i.e., yield strength of steel damper and phase transformation strength of SMA damper) on different responses parameters, such as the peak floor acceleration, peak floor interstory drift ratio, and peak floor residual displacement. Fig. 6 (a) shows the variation of the peak floor acceleration with respect to the normalized strength of the dampers. It is found that, with the increase in the normalized strength (normalized with respect to the weight of each floor of the building) of damper, top floor acceleration increases for both yield and SMA damper. This is due to the increase in rigidity of structure which leads to the stiffening of building structure, and thereby it causing more acceleration. Also, it can be observed that, the increase in peak floor acceleration is more pronounced for the yield damper retrofitted building than the SMA damper case. In comparison to yield damper, SMA damper reduces peak floor acceleration by maximum 28.4 %. Next, Fig. 6 (b) describes the effect of the change in normalized strength on the peak floor interstory drift ratio. It can be observed from Fig. 6 (b) that, the interstory story drift ratio reducing largely for yield damper, whereas in case of SMA damper the trend stays almost constant. Compare to the yield damper, SMA damper enhances maximum 37.2 % the floor displacement control efficiency. Fig. 6 (c) shows that, the reduction in the peak floor residual displacement is maximum 49.8 % more for SMA damper assisted building than yield damper. Here also, it can be observed that, variation in the peak floor residual displacement is much more for the yield damper retrofitted building than the SMA damper. Such a rather remarkable re-centring capacity of the SMA damper is due to the shape recovery property of super-elastic SMA, which is otherwise absent in yield damper. Another important observation is that, to obtain the similar level of peak floor displacement and residual floor displacement control efficiency, yield damper needs very high value of normalized strength than SMA damper, and this ultimately increases the floor acceleration. Thus, the SMA damper not only provides a better control efficiency than yield damper, at the same time SMA damper needs lesser amount of strength (i.e. less material), than the yield damper. Therefore, it can be concluded that, SMA damper provides of high level of response control efficiency at the low level of strength. Hence, due to this dual advantage, it expands the applicability of SMA damper over the yield damper, as seismic vibration control/ retrofitting device.

The effect of time period of the building is studied in Fig. 7. Due to increase in time period of building, the peak floor accelerations for all three systems (only building, yield damper retrofitter building, and the SMA damper retrofitted building) shows a decreasing trend, as depicted in Fig. 7 (a). SMA damper retrofitted building shows a maximum of 37.7 % reduction in peak floor acceleration than the yield damper retrofitted building. Also, at the lower time period of building structure, both the damper reduces peak floor acceleration at much faster rate than higher time period. But, after certain critical value of building time period, both the damper loses floor acceleration reduction capacity. However, compare to

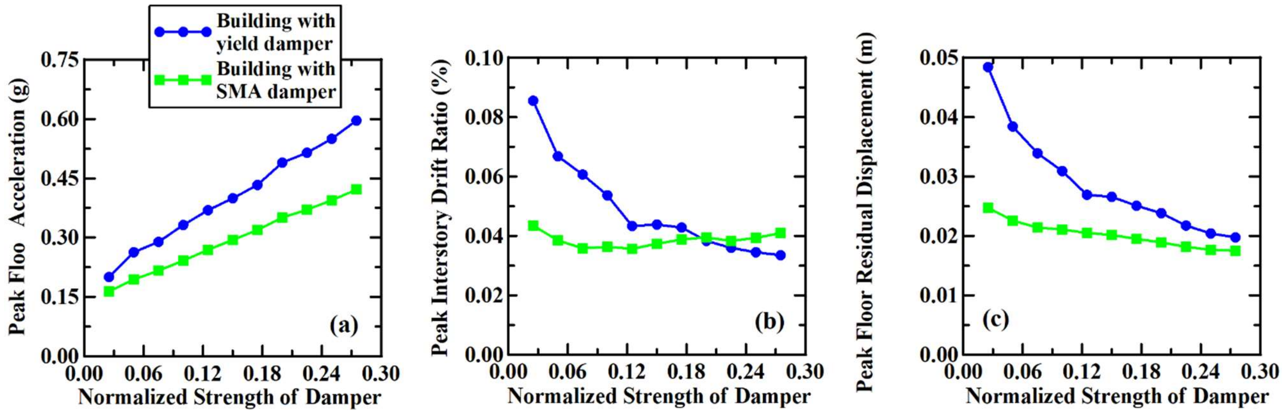

Fig. 6: Effect of variation of the normalized strength of yield and SMA damper on the (a) peak floor acceleration, (b) peak floor interstory drift ratio, and (c) peak floor residual displacement.

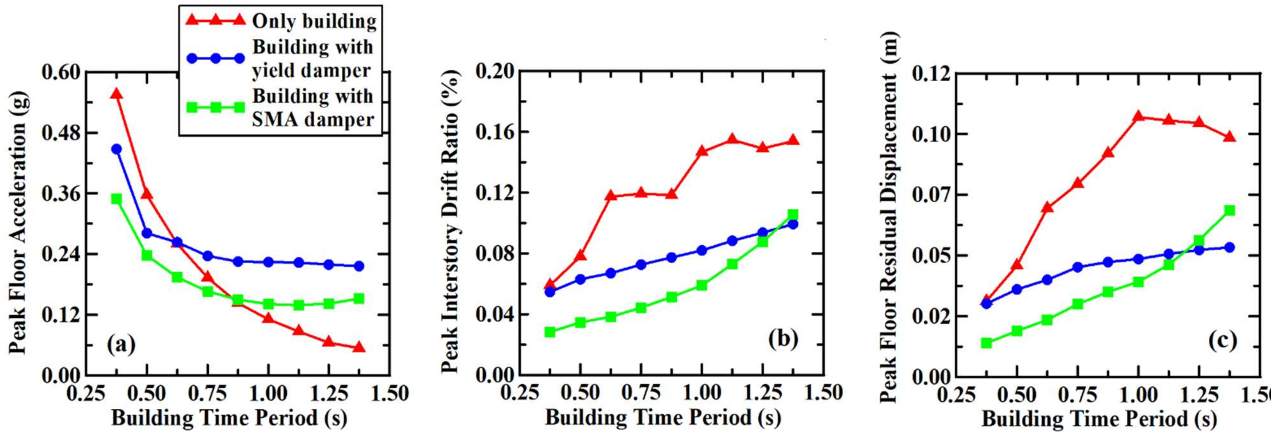

Fig.7: Effect of variation of the fundamental mode time period of building structure on the (a) peak floor acceleration, (b) peak floor interstory drift ratio, and (c) peak floor residual displacement.

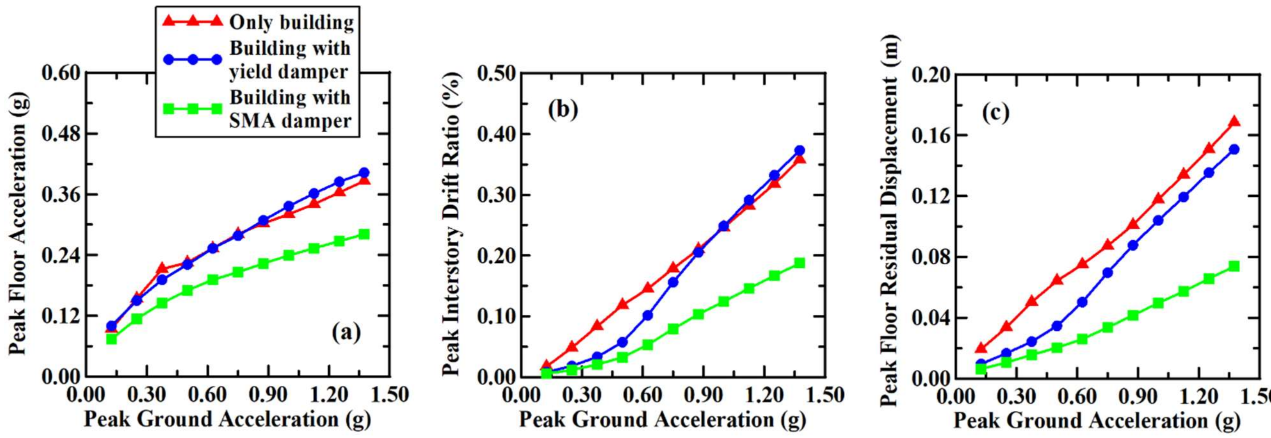

Fig. 8: Effect of variation of the peak ground acceleration on the (a) peak floor acceleration, (b) peak floor interstory drift ratio, and (c) peak floor residual displacement.

the yield damper, SMA damper provides higher acceleration control efficiency for a wider range of building time period. Fig. 7 (b) shows that, with increasing time period of building, the peak floor interstory drift ratio increases. Further, it can be seen that, when the time period of building is less, SMA damper is more promising, as well as effective than the yield damper. However, at higher time period of the building, yield damper provides comparable level of control efficiency as SMA damper. In comparison to yield damper, SMA damper provides 40.4 % more interstory drift ratio reduction in the retrofitted building. It can be found from Fig. 7 (c) that, due to the recentering capability, super-elastic SMA damper is able to reduce more (almost 54.1 %) peak residual floor displacement than yield damper. Here also, at lower value of building time period, variation in the peak residual floor displacement is more than that of the higher time period, and at higher time period yield damper reduces more residual displacement than the SMA damper.

In this study, it has been considered that structure and damper will show nonlinear force-deformation behaviour during the ground motion. This will provide large amount of hysteretic damping and dissipate significant part of seismic energy. Under such condition structural damping will not play significant role in seismic energy dissipation and thus, the variation in structure damping does not have any effect on dampers performance. This has been already demonstrated in other study on SMA damper [25].

Fig. 8 shows the scaling effect of the peak ground acceleration (PGA) on the response parameters i.e. on peak floor acceleration, peak interstory drift ratio, and peak floor residual displacement. With increasing value of PGA, all the response parameters show increasing trend. Variation of peak floor acceleration with PGA is shown in the Fig. 8 (a). Here yield damper retrofitted building does not provide any reduction in peak value of floor acceleration, whereas the SMA damper retrofitted building shows noticeable amount of reduction in the peak floor acceleration value. Compare to the yield damper, SMA damper provides up to maximum 30.4 % higher peak floor acceleration reduction. Fig. 8 (b) provides the variation of peak interstory drift ratio with respect to the PGA of the earthquake motions. In contrast to yield damper, SMA damper provided maximum 43.4% more reduction in the peak interstory drift ratio. Fig. 8 (c) shows the variation of peak residual floor displacement variation, where SMA damper provide higher control efficiency than yield damper, specifically at higher value of PGA. As can be observed from Fig. 8 (c) that, the SMA damper reduces up to maximum 52.4 % peak residual floor displacement than that of yield damper. An important observation is that, at lower value of PGA, both the damper provides sufficient reduction in all the response parameters. However, at higher value of PGA, yield damper loses its acceleration and displacement control efficiency and provides almost same value of peak floor acceleration and interstory drift ratio as the non-retrofitted building. Whereas, with increasing PGA, SMA damper increases the response control efficiency. Such an interesting phenomena is only observed in case of the super-elastic SMA damper because of the rate dependent behaviour of the SMA material, which is otherwise absent in yield damper material i.e. steel. It has been reported in other studies that, the hysteresis loop size (i.e. hysteresis energy dissipation capacity) of SMA increases with increasing loading/ strain rate [24]. Due to the scaling of ground motion, at high value of PGA, large amount of load comes to the damper, within a short time duration i.e. damper experiences higher magnitude of loading rate at the high value of PGA. Therefor due to the passive nature of yield damper, it is not able to dissipate sufficient part of imparted seismic energy. Thus, yield damper loses control efficiency, and this ultimately get reflected in terms of the high value of responses. On the other hand, with increasing PGA, loading rate increase and thus SMA damper provides higher seismic energy dissipation which ultimately causes reduction in the response parameters. Therefore, as compared to the yield damper, SMA damper can be used as retrofitting device for wide range of earthquakes. Thus, from all the above results it is clear that, compare to the yield damper, the SMA damper provided superior control efficiency and viable for wide range of application.

5. Conclusion

Present study compares the performance of SMA damper with the yield damper as the passive seismic vibration control device, in building structure. Responses are estimated using nonlinear dynamic response analysis, under 25 set of ground motions obtained from past near-fault and far-field earthquakes. Response analysis results show lesser floor responses (acceleration and displacement) for yield and SMA damper retrofitted building than the uncontrolled building. Further it has been observed that, for the selected ground motion, SMA dampers prove superior control efficiency over yield damper, via significantly reducing the floor acceleration and displacements of the nonlinear building. Also, compare to the yield damper, SMA damper significantly reduces the residual floor displacement, at the end of earthquake.

Performance of the dampers are evaluated under varying parameters like normalized strength of dampers, time period of the building structure, peak ground acceleration of the earthquake. Parametrical study results show that, compare to the yield damper, the SMA damper reduces floor peak acceleration by 14 % and interstory drift ratio by 38 % for the nonlinear building. Another extraordinary potential of SMA damper is that it's recentering capability, which is otherwise absent in case of yield damper. Compare to the yield damper, SMA damper reduces residual displacement by 47 %, and leaves almost very negligible permanent displacement in building. Parametric study results reveal that, for the similar level of control efficiency SMA damper requires much lower value of strength than the yield damper and at the same time provide sufficiently good acceleration and displacement reduction at low value of damper strength. This reduces the requirement of large volume of material, which ultimately increases the applicability of SMA damper over the yield damper. Further SMA damper provides very good control efficiency at high intensity (i.e. PGA) of seismic loading, whereas yield damper loses its control efficiency under the higher PGA ground motions. Thus, taken-together all the aforementioned results it can be stated that, SMA damper provides superior control efficiency over the yield damper, and therefore behaves much better seismic retrofitting device for building structure.

Acknowledgment

Authors' wants to acknowledge the financial support provided by the Department of Science and Technology (DST) of the Government of India, through the Start-up Research Grant (SRG/2020/000892) by the Science and Engineering Research Board (SERB).

Disclosures

Free Access to this article is sponsored by SARL ALPHA CRISTO INDUSTRIAL.

References

1. Mahin SA. Lessons from damage to steel buildings during the Northridge earthquake. Engineering Structures, 1998; 20(4–6): 261–270.
2. Dufka CL. The Mexico City Earthquake Disaster. Social Casework. 1988; 69(3): 162-170.
3. Kasai K, Maison BF. Building pounding damage during the 1989 Loma Prieta earthquake. Engineering Structures, 1997; 19(3): 195–207.
4. Javanmardi A, Ibrahim, Z, Ghaedi K, Ghadim, HB, Hanif MU. State - of - the - Art Review of Metallic Dampers: Testing, Development and Implementation. Archives of Computational Methods in Engineering, 2019; 27(2): 455–478.

5. Manchalwar A, Bakre SV. Optimization of Metallic Damper Location for Seismic Response Control. Journal of Vibration Engineering & Technologies, 2019; 7(3): 261–275.
6. Yamamoto M, Sone T. Damping systems that are effective over a wide range of displacement amplitudes using metallic yielding component and viscoelastic damper in series. Earthquake Engineering and Structural Dynamics, 2014; 43(14): 2097–2114.
7. Qian H, Li H, Song G, Guo W. Recentering shape memory alloy passive damper for structural vibration control. Mathematical Problems in Engineering, 2013; 2013: 963530.
8. Graesser EJ, Cozzarelli FA. Shape-Memory Alloys as New Materials for A seismic Isolation. Journal of Engineering Mechanics, 1991; 117(11): 2590–2608.
9. Menna C, Auricchio F, Asprone D. Applications of Shape Memory Alloys in Structural Engineering. Shape Memory Alloy Engineering, 2015; 369–403.
10. Li R, Ge H, Shu G. Parametric Study on Seismic Control Design of a New Type of SMA Damper Installed in a Frame-Type Bridge Pier. Journal of Aerospace Engineering, 2018; 31(2): 04017100.
11. Varughese K, El-hacha R. Experimental free vibrations test of steel braced frames reinforced with NiTi shape memory alloy wires. Structures, 2021; 29: 1165–1172.
12. Falahian A, Asadi P, Riahi HT, Haghy M. Seismic performance assessment of steel frames with shape memory alloy wire based dampers. The Structural Design of Tall and Special Buildings, 2020; 29(16): e1797.
13. Choi E, Nguyen HD, Jeon JS, Kang JW. Self-centering and damping devices using SMA dual rings. Smart Materials and Structures, 2019; 28: 085005.
14. Qiu C, Fang C, Liang D, Du X, Yam MC. Behavior and application of self-centering dampers equipped with buckling-restrained SMA bars. Smart Materials and Structures, 2020; 29: 035009.
15. Pereiro-Barceló J, Bonet JL. Ni-Ti SMA bars behaviour under compression. Construction and Building Materials, 2017; 155: 348–362.
16. Asfaw AM, Sherif MM, Xing G, Ozbulut OE. Experimental Investigation on Buckling and Post-buckling Behavior of Superelastic Shape Memory Alloy Bars. Journal of Materials Engineering and Performance, 2020; 29(5): 3127–3140.
17. Zhang Y, Zhu S. A shape memory alloy-based reusable hysteretic damper for seismic hazard mitigation. Smart Materials and Structures, 2007; 16(5): 1603–1613.
18. Zhang Y, Zhu S. Seismic response control of building structures with superelastic shape memory alloy wire dampers. Journal of Engineering Mechanics, 2008; 134(3): 240–251.
19. Miller DJ, Fahnestock LA, Eatherton MR. Development and experimental validation of a nickel-titanium shape memory alloy self-centering buckling-restrained brace. Engineering Structures, 2012; 40: 288–298.
20. Gur S, Frantziskonis GN, Mishra SK. Thermally modulated shape memory alloy friction pendulum (tmSMA-FP) for substantial near-fault earthquake structure protection. Structural Control and Health Monitoring, 2017; 24(11): e2021.
21. Gur S, Mishra SK, Frantziskonis GN. Thermo-mechanical strain rate–dependent behavior of shape memory alloys as vibration dampers and comparison to conventional dampers. Journal of Intelligent Material Systems and Structures, 2015; 27(9), 1250–1264.
22. Wen YK. Equivalent linearization for hysteretic systems under random excitation. Journal of Applied Mechanics, 1980; 47(1): 150–154.
23. Helm D, Haupt P. Shape memory behaviour: modelling within continuum thermomechanics. International Journal of Solids and Structures, 2003; 40(4): 827–849.
24. Gur S, Xie Y, DesRoches R. Seismic fragility analyses of steel building frames installed with superelastic shape memory alloy dampers: comparison with yielding dampers. Journal of Intelligent Material Systems and Structures, 2019; 30(18–19): 2670–2687.
25. Gur S, Mishra SK, Roy K. Stochastic seismic response of building with super-elastic damper. Mechanical System and Signal Processing, 2016; 72–73: 642–659.